Photopotentiation of the $GABA_A$ receptor with caged diazepam

Lorenzo Sansalone[a,1,2], Joshua Bratsch-Prince[b], Sicheng Tang[a], Burjor Captain[a], David D. Mott[b], and Françisco M. Raymo[a,2]

[a]Laboratory for Molecular Photonics, Department of Chemistry, University of Miami, Coral Gables, FL 33146; and [b]Department of Pharmacology, Physiology and Neuroscience, School of Medicine, University of South Carolina, Columbia, SC 29208

Edited by Ehud Y. Isacoff, University of California, Berkeley, CA, and approved September 11, 2019 (received for review February 15, 2019)

As the inhibitory γ-aminobutyric acid–ergic (GABAergic) transmission has a pivotal role in the central nervous system (CNS) and defective forms of its synapses are associated with serious neurological disorders, numerous versions of caged GABA and, more recently, photoswitchable ligands have been developed to investigate such transmission. While the complementary nature of these probes is evident, the mechanisms by which the GABA receptors can be photocontrolled have not been fully exploited. In fact, the ultimate need for specificity is critical for the proper synaptic exploration. No caged allosteric modulators of the $GABA_A$ receptor have been reported so far; to introduce such an investigational approach, we exploited the structural motifs of the benzodiazepinic scaffold to develop a photocaged version of diazepam (CD) that was tested on basolateral amygdala (BLa) pyramidal cells in mouse brain slices. CD is devoid of any intrinsic activity toward the $GABA_A$ receptor before irradiation. Importantly, CD is a photoreleasable $GABA_A$ receptor-positive allosteric modulator that offers a different probing mechanism compared to caged GABA and photoswitchable ligands. CD potentiates the inhibitory signaling by prolonging the decay time of postsynaptic GABAergic currents upon photoactivation. Additionally, no effect on presynaptic GABA release was recorded. We developed a photochemical technology to individually study the $GABA_A$ receptor, which specifically expands the toolbox available to study GABAergic synapses.

photopharmacology | IPSCs | epilepsy | benzodiazepines | GABA

It was November 15, 1963. The US Food and Drug Administration had just approved what would become an important drug milestone in the years to come: diazepam (DZP; first commercially marketed with the brand name of Valium) (1). The drug, belonging to the benzodiazepines (BDZs) class (2), successfully treated insomnia (3–5), anxiety disorders (6–8), epilepsy (9–11), muscle spasms (12), and alcohol withdrawal (13). Although novel and safer medications have been developed over the years, DZP still remains a fundamental treatment option; while the clinical use of the drug has been vastly exploited and, at a certain level, surpassed by better agents, its use in experimental neuropharmacology is still of cardinal importance. In fact, since the pioneering studies of Braestrup and Squires (14, 15) and Möhler and Okada (16) in 1977, which proved the existence of a unique binding site for BDZs in the central nervous system (CNS), many studies have been published depicting the specific mechanism of action of BDZs on neurons expressing γ-aminobutyric acid type A ($GABA_A$) receptors (17–20) and defining the fine neural processes pertaining to GABAergic transmission (21–26). It is not surprising that its involvement with many pathological conditions has progressively been described: From epilepsy to anxiety, association of the GABAergic system with schizophrenia (27), autism (28, 29), neuropathic pain (30), depression (31, 32), postoperative cognitive dysfunction (33), and many other conditions has been reported (34), and it is seriously increasing. In point of fact, about 25% of CNS neurons are estimated to be GABAergic (35); hence, alteration of this transmission has a critical impact on the whole-brain physiology. It is thus evident that despite the availability of hundreds of agonists and antagonists, the need for newer pharmacological tools to probe the GABAergic transmission, and shine light on poorly understood conditions, is of the utmost importance. Since the advent of photopharmacology (36–40), in a broader sense, several light-responsive probes have been reported and tested successfully. Most of the photopharmacological ligands acting on the GABA receptors belong to 2 different classes: (1) caged GABA probes and (2) photoswitchable ligands. From the first report of a caged version of GABA (41), many advances have been made to improve the physicochemical properties of the molecule (42–49), and thus the scope of the underlying research (50–54). However, the presence of antagonistic intrinsic activity of the caged molecule or the lack of specificity of GABA itself toward the different classes of GABA receptors (A, B, or A-ρ) limits their use. The only notable exception is represented by the recently reported cloaking technology developed by Ellis-Davies and coworkers (47, 55), which successfully removes the intrinsic antagonistic activity of the caged probe (up to 100 μM for G5-DEAC450-GABA and up to 2 mM for G3.5-BIST-GABA). Interestingly, the majority of the reported photoswitches inhibit the GABAergic functionality. A powerful genetically based strategy for the optical inhibition of virtually any specific α-subtypes of $GABA_A$ receptor in vitro and in vivo is represented by the LiGABARs (light-regulated

Significance

Anxiety, autism, epilepsy, and schizophrenia are just a few of the critical conditions associated with a dysfunctional γ-aminobutyric acid–ergic (GABAergic) system. Interrogation of such transmission is thus of ultimate importance for a better pathophysiological characterization of defective neuronal populations and proper treatment development. We describe here a probing mode designed to interrogate the GABAergic transmission. Specifically, we harnessed the photosensitive nature of a photoactivatable version of diazepam to specifically modulate the GABA type A ($GABA_A$) receptor kinetics upon photoirradiation. This technology allows the potentiation of GABAergic currents without affecting the receptor activation event operated by endogenous GABA. The important functional advance sets the basis for a specific explorative approach to investigate the pathological roles of $GABA_A$.

Author contributions: L.S., D.D.M., and F.M.R. designed research; L.S., J.B.-P., S.T., and B.C. performed research; L.S., J.B.-P., D.D.M., and F.M.R. analyzed data; and L.S., J.B.-P., D.D.M., and F.M.R. wrote the paper.

The authors declare no competing interest.

This article is a PNAS Direct Submission.

[1]Present address: Department of Neuroscience, Icahn School of Medicine at Mount Sinai, New York, NY 10029.

[2]To whom correspondence may be addressed. Email: l.sansalone@umiami.edu or fraymo@miami.edu.

This article contains supporting information online at www.pnas.org/lookup/suppl/doi:10.1073/pnas.1902383116/-/DCSupplemental.

First published October 1, 2019.

$GABA_A$ receptors) recently developed by Kramer and coworkers (56–58). Additionally, a gabazine azologue that photoreversibly antagonizes the $GABA_A$ receptor has been developed by Smart and Baker and coworkers (59). More recently, a photochromic ligand capable of blocking the anion-selective channel pore of several Cys-loop receptors, including $GABA_A$, $GABA_A$-ρ, and glycine receptors, has been reported (60). Finally, the only photochromic class of $GABA_A$ receptor potentiators is based on propofol azologues, which were independently reported by Trauner and coworkers (61) and Pepperberg and coworkers (62). The fine details on the many photoswitches developed can be found in 2 comprehensive reviews reported by Trauner and coworkers (40) and, more recently, by Paoletti et al. (63). Lastly, the only example of irreversible light-driven $GABA_A$ potentiation was reported by Mennerick and coworkers (64): Sustained light irradiation (30 to 60 s) of nitrobenzoxadiazole-tagged allopregnanolone generated the potentiation of GABAergic currents. However, the effect is not related to the biological activity of the photoirradiated molecule toward the receptor, but rather to what seems to be an irreversible photosensitizing reaction between a transient excited state of the molecule and cellular components. While it is clear that extensive work has been done for direct agonists and antagonists, just 1 class of photoresponsive-positive allosteric modulators (i.e., propofol azologues) has been reported, and we believe that potentiators of the GABAergic functionality specifically tailored toward the $GABA_A$ class could provide a novel way of probing synapses, as was also recently suggested (65). Here, we conceptualized a different approach in the specific photomodulation of the $GABA_A$ receptor kinetics without affecting its physiological activation operated by GABA. Surprised by the fact that no studies on caged BDZs have been published and aware of the pharmacoinvestigational value of the benzodiazepinic scaffold, we report here the design, synthesis, characterization, and electrophysiological evaluation on mouse brain slices of a photoactivable version of DZP, which we call caged diazepam (CD). A pictorial representation of the concept is reported in *SI Appendix*, Fig. S1.

Results

Design and Synthesis of CD. Although the benzodiazepinic scaffold is virtually "modifiable" in several positions, there are 2 very attractive motifs for caging: the amidic and iminic moieties. As DZP has the amidic nitrogen alkylated by a methyl group (Fig. 1*A*, **2**), the iminic element could be better exploited. Inspired by the early reports from 1971 at Hoffmann-La Roche (66), Upjohn (67), and Sankyo (68), where oxazolo and oxazino analogs of several BDZs were synthesized, we envisioned the possibility of installing a nitrobenzooxazine ring onto the BDZ scaffold (Fig. 1*A*, **1**), taking advantage of the reactive iminic carbon/nitrogen double bond. The rationale supporting the design of such a molecular frame is of double value. It is evident that the caged molecule should possess, at least in theory, no intrinsic activity toward the $GABA_A$ receptor, and analysis of the extensive and discrete list of BDZ structure–activity relationships (69–71) published over the years suggests that the introduction of such a heterocycle on the iminic part would alter the molecular geometry and shape sufficiently to suppress activity. Additionally, the reliable and extensive use of this caging motif for the synthesis of photoactivatable fluorophores, reported in recent bioimaging studies (72, 73), makes it very appealing in a photopharmacological scenario. In fact, the presence of a nitro functionality on the benzooxazine ring confers high photosensitivity to compound **1**, which can be used as a "light-sensitive prodrug" of DZP (Fig. 2). A solid synthetic protocol of 6 total steps was devised (Fig. 1*A* and synthetic scheme in *SI Appendix*, *Synthetic Procedures*): Chloroaminobenzophenone was reacted with bromoacetyl bromide to afford amidic derivative **3** in good yield. The following Delépine reaction and subsequent dehydrative cyclization provided nordazepam **4** in good yield. Deprotonation of the amidic nitrogen and alkylation with methyl iodide afforded **2** (DZP) in excellent yield. As shown by Sternbach and coworkers (66), BDZs can be reacted with epoxides in the presence of a Lewis acid to afford oxazolo analogs. It is then conceivable that an oxazine type of structure could be obtained by reacting DZP with a 2-bromomethylphenol derivative **5** without the need of an acid catalyst. The reaction should proceed in a 2-step manner, with the initial nucleophilic displacement of the halogen by the iminic nitrogen, followed by the oxygen attack on the quaternary iminic carbon to provide compound **1** (CD) in 60% yield. All of the compounds were characterized by NMR spectroscopy and electrospray ionization high-resolution mass spectrometry (*SI Appendix*, *Synthetic Procedures*). Additionally, single crystals of **1** were obtained, and X-ray diffraction analysis confirmed the presence of a locked benzooxazine moiety on the "once" iminic element of DZP (Fig. 1*B* and *SI Appendix*, Table S1). Moreover, superimposition of **1** and **2** crystal structures (*SI Appendix*, Fig. S2), aligned by the planes of the chlorinated rings, revealed a structural distortion induced by the oxazine heterocycle. Specifically, the phenylic quaternary carbons are out of plane of 0.6 Å with a twisted arrangement introduced by an intervening angle of 56°. Furthermore, the azepinic conformations are misplaced at C2, C3, and C5 (0.1 Å apart) and at N4 (0.4 Å away). Clearly, the introduction of the photoreactive moiety and the significant distortion from DZP native structure could be responsible for the lack of intrinsic activity reported for **1** (Fig. 3 *A* and *B*). However, introduction of the aromatic appendage affects the biophysical properties of **1**. In fact, while the dissolution of DZP in water is easily achievable, solubilization of CD in water-based media (deionized water or phosphate-buffered saline) was possible only with biologically incompatible amounts of organic auxiliary solvents (i.e., dimethyl sulfoxide > 1%). For this reason, we decided to use amphiphilic polymer **6** (Fig. 1*C*) as an effective solubilization aid. The presence of hydrophilic and hydrophobic chains in a polymeric unit allows the formation of self-assembled nanostructures in water-based environments, when the concentration of the polymer used is above the critical micelle concentration (CMC) (*ca.* 10^2 μg/mL) (74). The mixing of **1** and **6** in water results in the formation of micellar nanoconstructs (Fig. 1 *C*, *Right*), which can transport and deliver effectively the molecule of interest (74), as already demonstrated by recent studies in a biological context (72, 73).

Photophysical Characterization and Photolysis of CD. As the heterocyclic nitroaromatic appendage in **1** (Fig. 2*A*) was designed on the well-known nitrobenzyl-photosensitive platform, irradiation of **1** at activation wavelength (λ_{ac}) results in the irreversible fracture of the dihydro[1,3]oxazine moiety with the concomitant photogeneration of **2** (DZP) and rearrangement of the caging entity into the nitrosobenzaldehyde **7**, as depicted in Fig. 2*A*. The photochemical process can be followed spectroscopically (Fig. 2*B*), as shown by the evolution of the absorption spectrum over 3 min of irradiation of a **1** solution in MeCN (350 nm, 4.2 $mW \cdot cm^{-2}$). Note that the observed bathochromic shift for **1**, compared with **2**, is due to absorption by the nitrobenzyl moiety. Specifically, an increase in absorbance is recorded for 2 distinct bands at 320 nm and 375 nm. High-performance liquid chromatography analysis of an irradiated solution shows 3 resolved peaks for starting material **1** and photoproducts **2** and **7**. The peak for the former compound decreases in intensity over time, with a concomitant increase in the peaks of the latter species (Fig. 2*C* and *SI Appendix*, Fig. S3). The analysis of the temporal evolution of the concentration of **2** indicates the quantum yield of the photolytic process to be 0.07 (Fig. 2*C*, ϕ and *SI Appendix*, Fig. S5, *Left* and Table S2). The very same photolytic process can be performed within micelles of **6** in water (*SI Appendix*, Fig. S4), with a quantum yield of 0.06 (*SI Appendix*, Fig. S5, *Right* and Table S2). Additionally, the photolytic transformation of **1** into **2** and **7** was monitored by ^1H NMR in CD_3CN (Fig. 2*D* and *SI Appendix*, Fig. S6). A singlet for the methyl protons of **2** appears

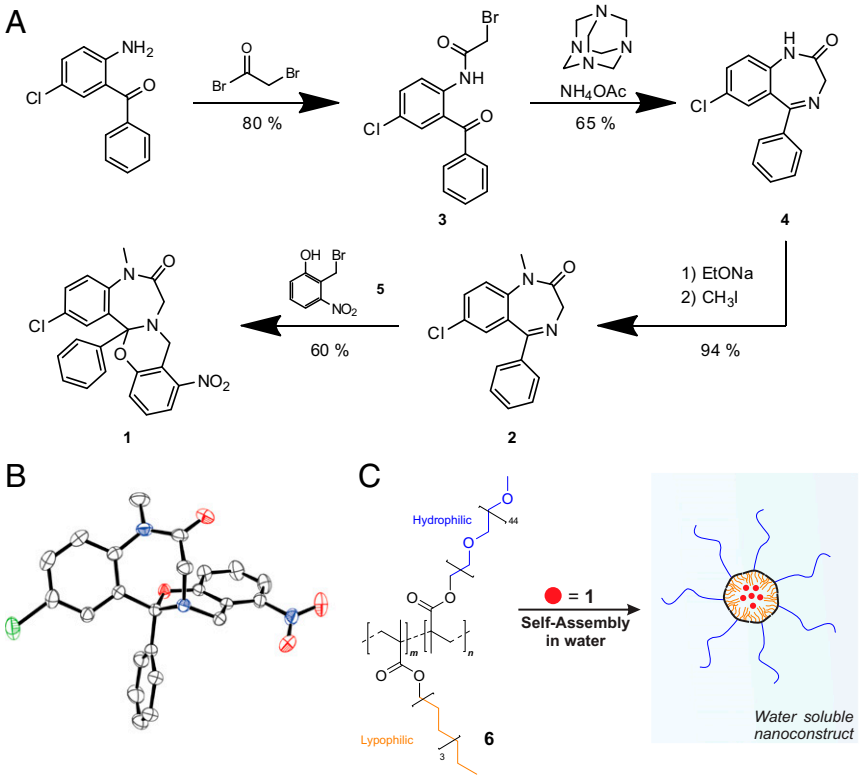

Fig. 1. (*A*) Synthetic scheme for the preparation of compound **1**: The aromatic chloroamino ketone is reacted with bromoacetylbromide to afford the bromomethyl derivative **3** in 80% yield. The subsequent amination with methenamine and acidic dehydrative cyclization affords **4** in 65% yield over 2 steps. Nordazepam **4** is then deprotonated with sodium ethoxide and reacted with methyl iodide to afford DZP **2** in 94% yield. The installation of the oxazine ring is performed, reacting DZP with the bromomethylnitrophenolic derivative **5** to afford the final product **1** in 60% yield. (*B*) Oak Ridge Thermal Ellipsoid Plot (40% thermal ellipsoid probability) representation of the geometry adopted by **1** in a single crystal (carbon [gray], oxygen [red], nitrogen [blue], chorine [green]). (*C*, *Left*) Structure of amphiphilic polymer **6** with relative ratio of hydrophobic-to-hydrophilic chains per polymer unit. (*C*, *Right*) Pictorial representation of a micellar self-assembled unit containing **1**.

at 3.32 parts per million (ppm) and increases in intensity with the photolytic transformations, while that of the methyl protons of **1** at 3.26 ppm decreases. Similarly, the peaks for the AB system at 3.63 ppm (center of the AB system) for the pair of diastereotopic protons adjacent to the carbonyl group of **1** decrease, with a concomitant increase in those of **2** at 4.19 ppm (center of the AB system). Finally, the decrease in intensity of the AB system for the diastereotopic methylenic protons of the oxazine ring at 4.43 ppm (center of the AB system) and the appearance and growth of a singlet at 10.24 ppm for the formyl proton of **7** confirm the photoinduced generation of this species as well.

Electrophysiological Evaluation of CD in Brain Slices. As previously mentioned, the analysis of the superimposed structures of CD (Fig. 1*A*, **1**) and DZP (Fig. 1*A*, **2**) suggested a virtual change in binding mode toward the BDZ binding pocket of the $GABA_A$ receptor (*SI Appendix*, Fig. S2). In order to determine the presence of any possible intrinsic activity of CD on the latter, a solution of the same (50 μM) was tested examining GABAergic activity in murine pyramidal cells in the basolateral amygdala (BLa; Fig. 3*F*) using whole-cell brain slice electrophysiology in the absence of light: No significant difference in the amplitude or decay of evoked GABAergic inhibitory postsynaptic currents (IPSCs) was detected compared with baseline (Fig. 3*A*, blue trace and Fig. 3*B*, blue bars), which led us to the assumption that CD is devoid of any BDZ-like activity, as well as any antagonistic or neurotoxic effect at such a concentration. Moreover, the amphiphilic carrier **6** (Fig. 1*C*), with or without light (λ_{ac} = 365 nm), did not significantly affect the amplitude or the decay of evoked IPSCs at a 250 μg/mL loading (Fig. 3*B*, black bars and *SI Appendix*, Fig. S7, *Bottom*), as expected. Finally, to confirm the lack activity of the nitroso photoproduct **7** (Fig. 2*A*), NBA (a nitrobenzyl alcohol derivative) was chosen as model cage as, upon its irradiation (λ_{ac} = 365 nm), water and NOB (a nitrosobenzaldehyde derivative) are released in situ (Fig. 3*E*). Once again, no significant difference in channel activity was detected when compared with the NBA baseline (Fig. 3 *A*, orange trace and *B*, orange bars). These results ruled out any influence from the polymeric carrier and the rearranged photochemical product on the evoked IPSCs, and also demonstrated that the ultraviolet (UV) light pulse itself had no effect. Thus, these experiments paved the road for CD testing. Application and equilibration of a nanomicellar solution of CD on BLa neurons, followed by a single light pulse (1 s, λ_{ac} = 365 nm, 2.87 mW/mm^2), significantly potentiated the decay of evoked IPSCs compared with CD baseline (**P < 0.01; Fig. 3 *C*, blue trace and *D*, blue bars). Likewise, application of a solution of DZP (1 μM), without light irradiation, resulted in the same decay potentiation pattern observed for the irradiated CD (*P < 0.05; Fig. 3 *C*, red trace and *D*, red bars), as has been previously reported in BLa pyramidal cells (75). In contrast, irradiation of a solution of CD, in the presence of the selective BDZ receptor antagonist flumazenil (10 μM), failed to cause any increase in decay time (Fig. 3*D*, gray bars and *SI Appendix*, Fig. S7, *Top*). Finally, both the irradiated CD and DZP did not significantly affect the amplitude of evoked IPSCs.

Kinetics Effects and Correlation between Irradiated CD and DZP. Increasing the irradiation time of a CD solution results in a higher photogeneration of DZP (Fig. 2*C* and *SI Appendix*, Fig. S5) and, translating the concept in a biological scenario, generates an increase in the decay time of evoked IPSCs (Fig. 4 *A*, *Top Left* and

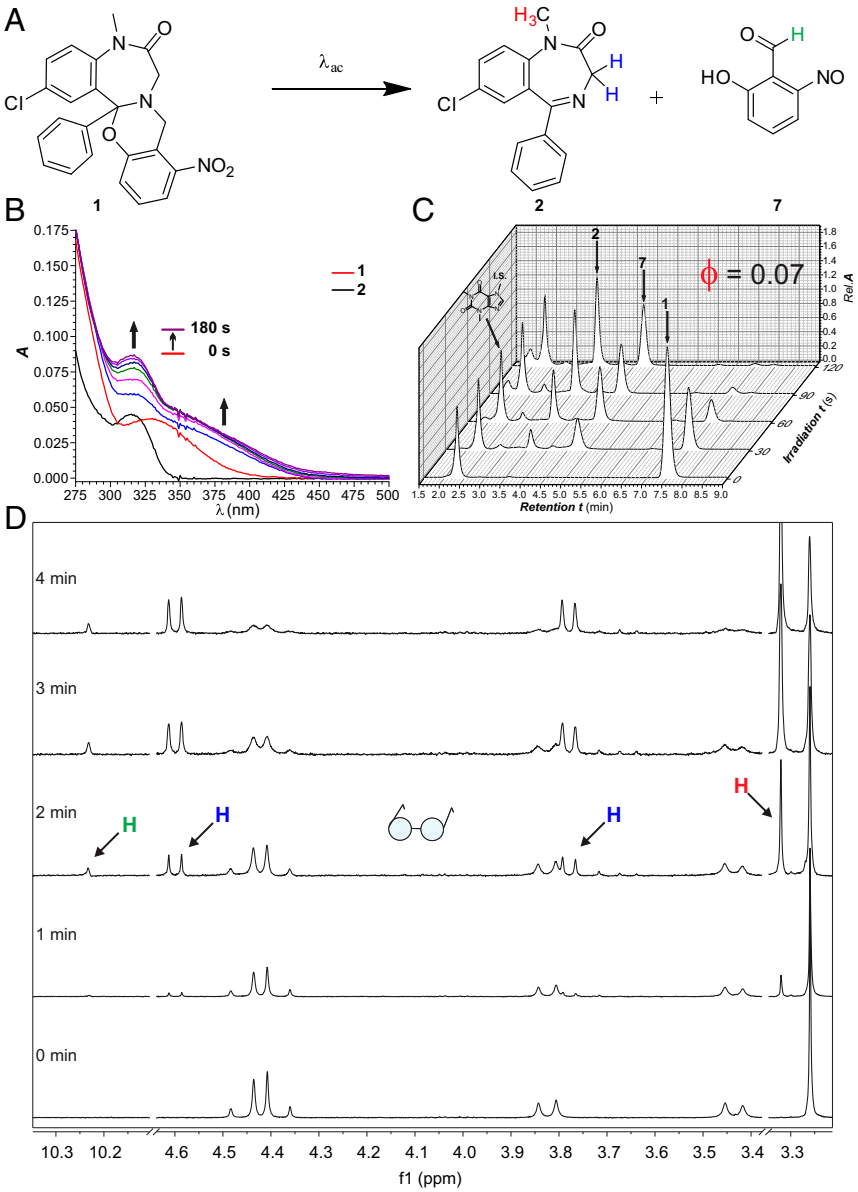

Fig. 2. (*A*) Chemical structures of reactant **1** and photoproducts **2** and **7** obtained upon irradiation of a MeCN solution of **1** (350 nm, 4.2 mW·cm^{-2}). (*B*) Absorption (*A*) spectra (MeCN, 20 °C, 20 μM) recorded before and during the photolysis of **1** for 3 min and of the isolated product (**2**). (*C*) High-performance liquid chromatography traces [1.0 mL·min^{-1}, C18 EVO, MeCN/H_2O (70:30, vol/vol), 254 nm] recorded before and during the photolysis (350 nm, 4.2 mW^{-2}) of a MeCN solution of **1**. Rel. A = relative absorption; *t* = time. (*D*) Evolution of a ^{1}H NMR spectrum of a CD_3CN solution of **1** before (0 min) and after (1 to 4 min) photolysis (350 nm, 4.2 mW^{-2}). Hydrogen (H) atoms are color-coded in the structure of **2**.

Bottom). The same effect was obtained by treating BLa pyramidal cells with increasing concentrations of DZP (Fig. 4 *A*, *Top Center*, *Top Right*, and *Bottom*). The graph shown in Fig. 4*B* correlates the increase in irradiation time of CD-treated BLa pyramidal cells (365 nm, 2.87 mW/mm^2) or the increase in concentration of DZP treatment to the decay time of evoked IPSCs. The 2 curves and the kinetic parameters of the currents in CD-treated cells (Fig. 4 *A*, *Bottom* and *SI Appendix*, Table S3) indicated an increase in decay time from 10.23 to 12.57 ms and from 11.93 to 19.60 ms, with respective irradiation times of 100 and 1,000 ms (compared with baseline). Specifically, a 23% increase was obtained for the shortest illumination time, while a 64% increase was recorded for the longer one. Correspondingly, in DZP-treated cells, increases of 17% and 56% were recorded when the respective concentrations used were 0.1 μM and 1 μM compared with baseline (Fig. 4 *A*, *Bottom*). Additionally, no significant alteration of the rise time or amplitude of evoked IPSCs was recorded for either treated group (*SI Appendix*, Table S3).

CD Rapidly Alters IPSC Kinetics by Acting on Postsynaptic GABA Receptors. We evaluated the influence of irradiated CD on miniature IPSCs (mIPSCs) to determine the time course of uncaging of CD and whether the effects occurred pre- or postsynaptically. Fig. 5 summarizes the properties of CD: The increase in decay time of mIPSCs is clearly visible after a 1-s pulse of 365 nm of light (2.87 mW/mm^2; Fig. 5*A*, blue dot). The mIPSCs are terminated by application of bicuculline, a $GABA_A$ receptor antagonist. Fig. 5*B* reports the averaged decay values for mIPSCs in 1-s bins during the 5 s prior to and 10 s after the UV light pulse. The mIPSC decay is potentiated by the first 1-s bin, reflecting the rapid (millisecond) on-rate for the uncaging effect after UV light. Note that the mIPSC recorded 200 ms after the light pulse is already potentiated.

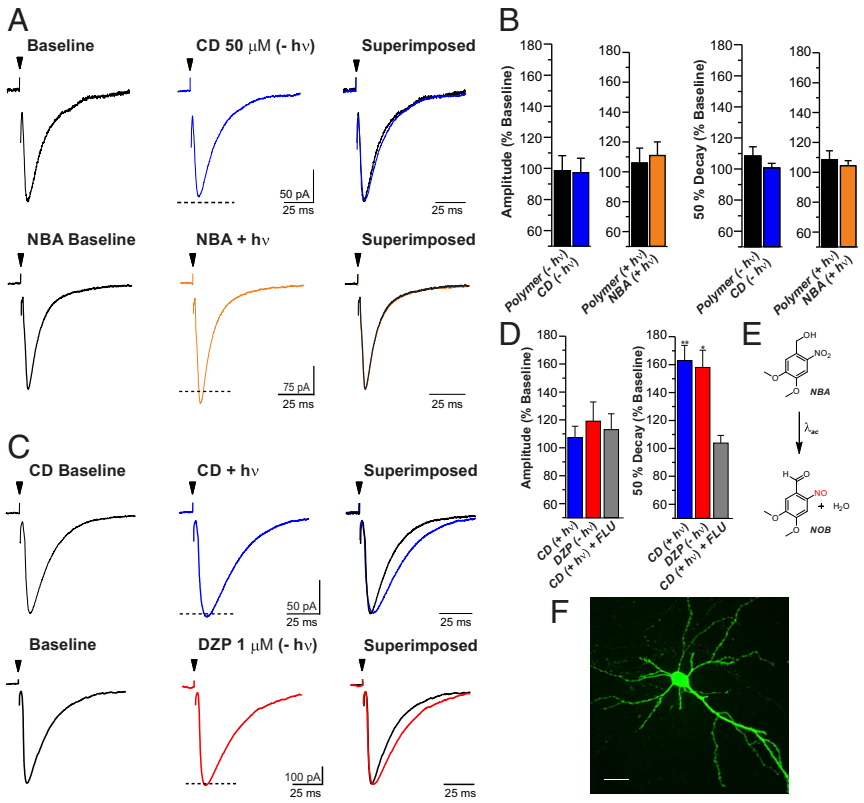

Fig. 3. (A, *Top*) Representative traces of evoked (arrowheads) GABAergic IPSCs in BLa pyramidal cells at baseline (*Left*) and after the addition of CD (50 μM, *Center*). + **hν** = with irradiation; - **hν** = without irradiation. (*Right*) IPSCs from baseline and after the addition of CD were superimposed to show the similarity in response in the different conditions. (*A*, *Bottom*) Representative traces of evoked (arrowheads) GABAergic IPSCs in BLa pyramidal cells after the addition of NBA (50 μM, *Left*) and after irradiation of the same (1 s, 365 nm, 2.87 mW/mm^2, *Center*). (*Right*) IPSCs from NBA baseline and irradiated NBA were superimposed to show the similarity in response in the different conditions. (*B*) Amplitude (*Left*) and decay (*Right*) change in percentage compared with baseline after polymer application (0.25 mg/mL, $n = 8$ cells, 4 animals), CD application (50 μM, $n = 5$ cells, 3 animals), polymer irradiation (1 s, 365 nm, 2.87 mW/mm^2, $n = 8$ cells, 4 animals) and NBA irradiation ($n = 6$ cells, 4 animals). (*C*, *Top*) Representative traces of evoked (arrowheads) GABAergic IPSCs in BLa pyramidal cells after the addition of CD (50 μM, *Left*) and after irradiation of the same (1 s, 365 nm, 2.87 mW/mm^2, *Center*). (*Right*) IPSCs from CD baseline and irradiated CD were superimposed to show the difference in response. (*C*, *Bottom*) Representative traces of evoked (arrowheads) GABAergic IPSCs in BLa pyramidal cells at baseline (*Left*) and after the addition of DZP (1 μM, *Center*). (*Right*) IPSCs from CD baseline and DZP were superimposed to show the difference in response. (*D*) Amplitude (*Left*) and decay (*Right*) change in percentage compared with baseline after CD application and irradiation ($n = 5$ cells, 3 animals), DZP application ($n = 5$ cells, 3 animals), and CD (50 μM) + flumazenil (FLU; 10 μM) application and irradiation (1 s, 365 nm, 2.87 mW/mm^2, $n = 5$ cells, 4 animals). All evoked stimulation artifacts were truncated for clarity. *$P < 0.05$; **$P < 0.01$. (*E*) Illustrated photogeneration of water and NOB (a nitrosobenzaldehyde derivative) from the model compound NBA when irradiated with UV light (1 s, 365 nm, 2.87 mW/mm^2). (*F*) Example of a recorded BLa pyramidal cell. (Scale bar: 25 μm.)

Fig. 5 *C* and *D* reports the averaged mIPSCs for irradiated CD and DZP. Cumulative probability histograms were generated for mIPSC kinetics in CD (60 s pre- and 10 s post-UV light) and bath-applied DZP (60 s of baseline and 60 s in 1 μM DZP). The mIPSCs were evaluated for 10 s following UV light because the effect of photogenerated DZP on mIPSC kinetics was stable during this period (Fig. 5*B*) due to the kinetics of drug removal from the recording chamber. This analysis showed a significant increase in mIPSC decay time after irradiation of CD or after application of DZP, as denoted by the rightward shift for all of the events (Fig. 5 *C* and *D*, *Right Top*). No significant difference was detected in amplitude or frequency of mIPSC events, suggesting irradiated CD, like DZP, is only acting on the postsynaptic $GABA_A$ receptor and is not acting on presynaptic GABA release (Fig. 5 *C*, *Right Bottom Left* and *Right* and *D*, *Right Bottom Left* and *Right*).

Discussion

The development of a photoactivatable allosteric modulator represents a different approach for the optical control of GABA receptors that works in concert with the endogenous agonist. Optical receptor modulation may thus produce different effects on GABAergic signaling compared with direct receptor activation (discussed below). In addition, for in vitro investigation of GABAergic transmission, CD displays 2 main advantages over caged GABA compounds in that DZP is specific just for $GABA_A$ receptors, whereas caged GABA compounds can activate $GABA_A$, $GABA_B$, and $GABA_A$-ρ receptors upon irradiation. This would become important for the exploration of synapses that possess both $GABA_A$ and $GABA_B$ receptors, as photoreleased GABA would act on both, favoring the cross-talk. In fact, activation of the single receptor results in different signaling outcomes compared with the coactivation, as was recently reported (76–78). Furthermore, at a concentration appropriate for photolysis, CD is biologically inert toward its target $GABA_A$ receptors. In contrast, most caged GABA compounds are antagonistic toward $GABA_A$ receptors at concentrations required for effective photolysis in brain tissue, with the only exception represented by the recently developed cloaked caged GABA (47, 55). Finally, while propofol azologues offer a way to optically control the receptor, the immediate effect upon application is potentiation without the need of light, thus behaving as classic allosteric modulators. The practical advantage is the effect reversal upon UV/Visible light (360 to 450 nm) irradiation; hence, these azologues offer a functional way

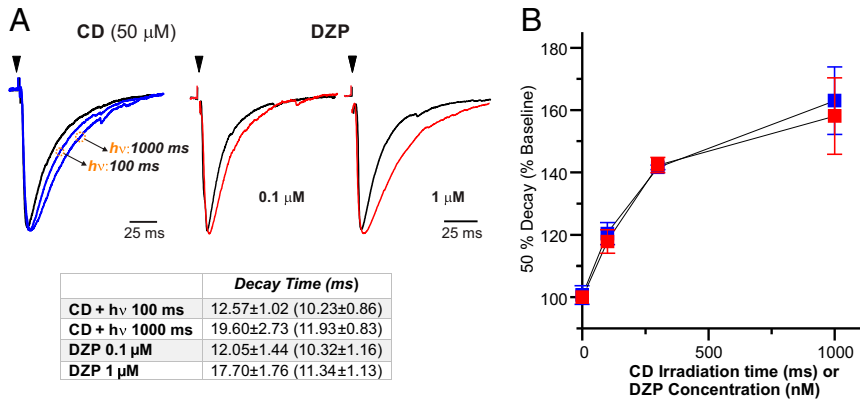

	Decay Time (ms)
CD + hν 100 ms	12.57±1.02 (10.23±0.86)
CD + hν 1000 ms	19.60±2.73 (11.93±0.83)
DZP 0.1 μM	12.05±1.44 (10.32±1.16)
DZP 1 μM	17.70±1.76 (11.34±1.13)

Fig. 4. (*A*, *Left*) Representative traces of evoked (arrowhead) GABAergic IPSCs in BLa pyramidal cells after the addition of CD (50 μM) followed by different irradiation times (100 ms, $n = 5$ cells, 3 animals; 1,000 ms, $n = 5$ cells, 3 animals). (*A*, *Top Center* and *Top Right*) Representative traces of evoked (arrowheads) GABAergic IPSCs in BLa pyramidal cells after the addition of DZP at different concentrations (0.1 μM, $n = 5$ cells, 4 animals; 1 μM, $n = 5$ cells, 3 animals). + **hν** = with irradiation. (*A, Bottom*) Table shows averaged decay times with SEM for GABAergic IPSCs in BLa pyramidal cells after the irradiation of CD-treated cells (50 mM, 365 nm, 2.87 mW/mm^2) or after DZP treatment. The values in parentheses are from baseline. (*B*) Overlapping traces of the effect on decay time for irradiated CD and DZP at increasing time or concentration.

to modulate the channel activity. CD, instead, allows potentiation of the receptor just upon irradiation as it is completely inert before photoactivation.

CD also holds an advantage over other methods of DZP application to brain slices, such as fast perfusion, for experiments studying the role of $GABA_A$ receptors in local circuits or inhibition onto single cells. Using whole-field photolysis, DZP can be uncaged simultaneously and rapidly across all GABA receptors in a local circuit, enabling study of the effects of $GABA_A$ receptors in that circuit. In contrast, fast perfusion (e.g., puffer pipette) typically applies DZP to a focal area, relying upon diffusion to carry the drug to receptors further away. Thus, receptors in the circuit are activated to different extents and at different times. Fast perfusion is also limited by steady-state diffusion of DZP from the puffer pipette, as well as potential pressure artifacts during drug application. UV illumination of CD-treated BLa pyramidal cells generated DZP proportional to the irradiation time and with a quantum yield of 0.07. For a given quantum yield, the

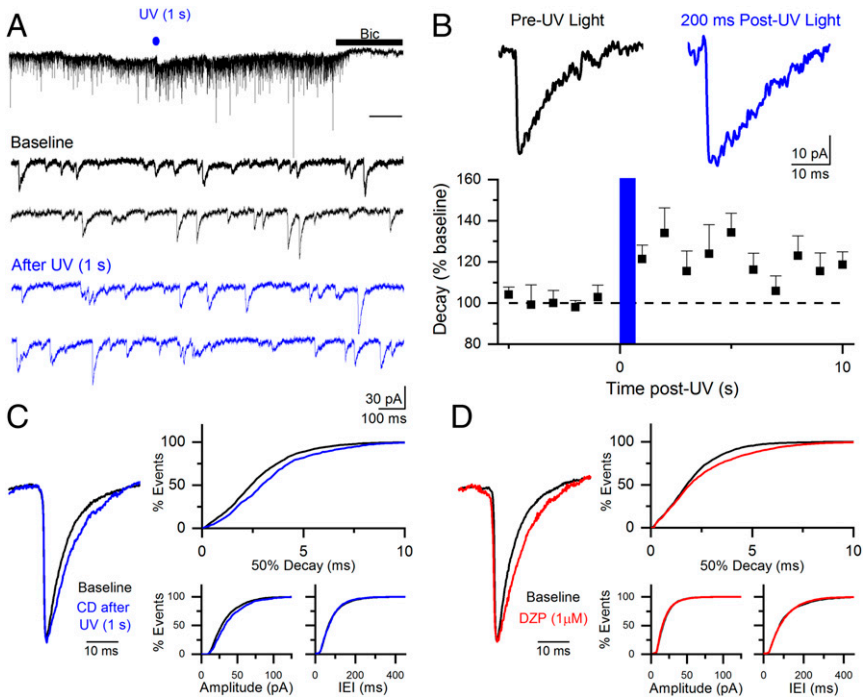

Fig. 5. (*A*) Representative traces of mIPSCs in a CD-treated (50 μM) BLa pyramidal cell before and after a 1-s pulse of UV light ($n = 6$ cells, 3 animals, 2.87 mW/mm^2; blue dot). Bic = bicuculline. (*B*) Average decay values of mIPSCs in 1-s bins in each of the 5 s before and 10 s after the UV light pulse to show the effect of CD on a millisecond time scale after the end of the UV light pulse. An example mIPSC from before (black trace) and 200 ms after the end of (blue trace) UV light highlights the quick onset of this effect. (*C*, *Left*) mIPSCs 60 s before (black trace) and 10 s after (blue trace) light irradiation in CD were averaged and superimposed. (*C*, *Right*) Cumulative probability diagram for decay (*Top*) shows a rightward shift after UV light irradiation, with no significant shift in amplitude (*Bottom Left*) or interevent interval (IEI; *Bottom Right*). (*D*, *Left*) Bath application of DZP (1 μM, $n = 5$ cells, 3 animals) shows a similar effect on mIPSCs. (*D*, *Right*) Cumulative probability diagram for decay (*Top*) shows a rightward shift after DZP application, with no significant shift in amplitude (*Bottom Left*) or interevent interval (*Bottom Right*).

photogeneration of DZP depends upon a number of factors, including the duration of illumination and the concentration of CD. The high affinity of DZP for the BDZ site on the $GABA_A$ receptor enabled the use of a substantially lower concentration (50 μM) of CD than the millimolar concentrations typically used for caged GABA. The use of this lower concentration of CD (50 μM) minimizes potential problems, such as concentration-dependent off-target effects and inner filter effects (79). Accordingly, with this concentration of CD, varying the UV light-pulse duration from 100 to 1,000 ms produced effects on the $GABA_A$ IPSCs similar to those produced by bath application of 100 to 1,000 nM DZP (DZP half maximal effective concentration ~ 120 nM) (80).

Repeated UV light pulses generated reproducible effects on IPSC kinetics. In addition, the on-rate of the effect of CD on IPSC decay was rapid and occurred within 200 ms after the light pulse. However, the overall time course of the response to CD reflects the whole-field illumination technique used in the present study. This form of illumination rapidly and simultaneously exposes much of the recorded cell to DZP. Once photogenerated, DZP relies on diffusion away from the site of action and washout to terminate its effect. Thus, while the on-rate of the effect of CD was rapid, the duration of the effect following the light pulse could last for tens of seconds and was dependent upon the kinetics of drug removal from the recording chamber. The 2-photon (2P) cross-section of the caging motif in CD is lower than 0.01 Goeppert Mayer (GM) (81); thus, probing a useful biological spatial resolution would require the chemical modification of the cage. Having defined here the structure/activity principles to develop photocaged BDZs will lead to future studies with 2P-sensitive cages.

While GABA produces a direct increase in GABAergic current (82), BDZs modulate the kinetics of receptor activation by endogenous agonists. The effect of BDZs on IPSC amplitude and kinetics at a given synapse depends upon synaptic $GABA_A$ receptor occupancy (83). Thus, in the present study in adult mouse BLa, both photogenerated DZP and bath-applied DZP prolonged the mIPSC decay but had no significant effect on mIPSC amplitude (Fig. 5). While the effects of DZP on mIPSCs in BLa have not previously been reported, the absence of an effect of BDZs on amplitude is in agreement with several previous studies in the hippocampal formation (84–86). The lack of an effect on amplitude is consistent with the presence of a saturating concentration of GABA in the synaptic cleft relative to the number of GABA receptors (87). DZP, which increases the on-rate of steady-state GABA binding to the receptor (88, 89), prolongs the decay of the mIPSC, but not the amplitude, as the synaptic receptors are already saturated with GABA. DZP also significantly prolonged the decay of the evoked IPSC. However, in contrast to its lack of effect on mIPSC amplitude (Fig. 5 *D*, *Right Bottom Left*), DZP caused a slight apparent increase in the amplitude of the evoked IPSC. This effect varied between cells but, on average, was not significant (Fig. 3*D*). In the hippocampus, the DZP-induced increase in amplitude of the evoked IPSC has been attributed to jitter in the timing of the underlying IPSCs, originating from individual synapses activated by the stimulus. DZP prolongs these individual mIPSCs, resulting in an increase in the amplitude of the compound-evoked IPSC (87). In the BLa, Kang-Park et al. (75) reported that DZP caused a significant increase in evoked IPSC amplitude greater than that observed in the present study. This dissimilarity may be attributed to differences in the species or ages of the animals used in that study (16- to 20-d-old rats) and the present study (35- to 56-d-old mice). DZP modulation of mIPSC amplitude is age-dependent and is preferentially observed in juvenile animals (90). DZP modulation of IPSC amplitude has also been reported to be temperature-dependent (91).

GABAergic transmission is critical for the temporally precise activity of neuronal circuits and the synchronized oscillatory activity of neuronal populations (92). GABAergic defects in these circuits contribute to a variety of neurological disorders, including anxiety, autism, epilepsy, and schizophrenia. Development of photochromic modulators capable of regulating receptor activity provides a powerful tool for investigation of the role of GABA receptors in these circuits. CD differs from these compounds in its site of action on the $GABA_A$ receptor and mode of action, as it is biologically inert until exposed to UV light. In particular, CD will enable the study of GABAergic transmission in local circuits in vitro. In vivo, this compound opens the possibility to explore associations between neuronal activity in specific brain regions and behavior. Through the use of implanted optical fibers, CD could allow for investigation of the effect of regional photopotentiation of GABAergic transmission on behaviors such as anxiety or epileptic seizures in vivo, as has been reported with RuBi-GABA by Rothman and Yuste and coworkers (54). However, the known antagonistic activity and neuronal toxicity of the used probe limit the extent of research. Indeed, CD could be useful in a similar scenario. Specifically, regional potentiation of GABAergic transmission in a seizure focus, produced by the diffusible modulator combined with focal light stimulation, could result in the optical termination of the seizure and enable a deeper understanding of the pathophysiology of epileptic conditions.

Conclusion

We have demonstrated that the benzodiazepinic scaffold can be chemically engineered to obtain photoactivatable positive allosteric modulators of the $GABA_A$ receptor (CD). Using whole-cell electrophysiology on murine BLa pyramidal cells, we found that CD (50 μM) potentiated $GABA_A$ IPSCs in a photoinducible manner. Upon exposure to UV light (365 nm, 2.87 mW/mm^2), CD produced a rapid (millisecond) prolongation of IPSC decay, reflecting the action of photoreleased DZP at the BDZ site of the $GABA_A$ receptor. Furthermore, CD did not affect mIPSC frequency, suggesting that it did not alter presynaptic GABA release and that its effects on GABAergic transmission were entirely postsynaptic at the $GABA_A$ receptor. CD is biologically inert toward the receptor before activation (i.e., no agonistic or antagonistic activity was recorded). This probing technology can be applied to brain slices without any genetic manipulation. CD thus represents a photoactivatable ligand of the BDZ site capable of specific positive allosteric modulation of the $GABA_A$ receptor. Finally, we set the physicochemical basis for the future development of photoactivatable compounds based on BDZs with preferential affinity for specific $GABA_A$ receptor subtypes (e.g., α1, α2, α3, α5). These compounds could assist in defining the roles of specific $GABA_A$ receptor subtypes in the regulation of cognitive and emotional neural processes.

Materials and Methods

Chemicals. The synthetic procedure and spectroscopical characterization for CD can be found in *SI Appendix*. Compounds **5** and **6** were synthesized as previously described (74).

Photolytic Procedure. The samples were irradiated in aerated solutions with a Luzchem Research LZC-4V photoreactor, operating at 350 nm (4.2 $mW \cdot cm^{-2}$). The corresponding quantum yields were determined with a potassium ferrioxalate actinometer according to an established procedure (*SI Appendix*).

Brain Slices. All animal care and use procedures were carried out in accordance with protocols written under the guidelines of the National Institutes of Health *Guide for the Care and Use of Laboratory Animals* (93) and approved by the Institutional Animal Care and Use Committee at the University of South Carolina. Brain slices were prepared from C57BL/6J male mice that were 5 to 8 wk old.

Electrophysiology. All IPSCs were isolated in BLa pyramidal neurons using a mixture of glutamate receptor antagonists (D-2-aminophosphonovaleric acid, 50 μM and 6-cyano-7-nitroquinoxaline-2,3-dione, 50 μM) in the recording

solution. Currents were recorded at −70 mV using internal solutions with high chloride (*SI Appendix*). Evoked IPSCs were produced by a stimulating electrode placed locally near the recorded cell. In experiments recording mIPSCs, 1 μM tetrodotoxin was added to the mixture. Input and series resistance were monitored throughout all experiments, and recordings in which either changed significantly were discarded. At the conclusion of all experiments, 30 μM bicuculline methochloride was applied to confirm that responses were mediated by $GABA_A$ receptors.

Photoactivation. Experiments and drug preparations involving UV light were performed in the dark. Drugs were allowed to wash on for at least 2 min before UV light was applied. UV light (365-nm light-emitting diode, pE-4000; CoolLED) was applied through a 40× objective (Olympus BX51WI, 0.8 numerical aperture) focused over the recorded cell. Light power was controlled by the control panel of the pE-4000 instrument, while the duration was controlled via pClamp10 software. The light power was measured with a photometer (S120VC; Thorlabs) prior to the experiment.

Crystallographic data, supporting figures, slice protocols, and statistical methods are available in *SI Appendix*.

ACKNOWLEDGMENTS. This work was supported by the National Science Foundation (Grant CHE-1505885 to F.M.R.) and by the NIH (Grant R01 MH104638 to D.D.M.).

1. N. E. Calcaterra, J. C. Barrow, Classics in chemical neuroscience: Diazepam (valium). *ACS Chem. Neurosci.* **5**, 253–260 (2014).
2. G. A. Archer, L. H. Sternbach, Chemistry of benzodiazepines. *Chem. Rev.* **68**, 747–784 (1968).
3. J. C. Gillin, W. F. Byerley, Drug therapy: The diagnosis and management of insomnia. *N. Engl. J. Med.* **322**, 239–248 (1990).
4. P. Reading, S. J. Wilson, "Pharmacological treatment of insomnia and parasomnias" in *Sleep Disorders in Neurology*, S. Overeem, P. Reading, Eds. (John Wiley & Sons Ltd, 2018), pp. 61–72.
5. M. S. Sastre y Hernández, H. D. Hentschel, K. Fichte, Comparative efficacy of lormetazepam (Noctamid) and diazepam (Valium) in 100 out-patients with insomnia. *J. Int. Med. Res.* **9**, 199–202 (1981).
6. S. M. Stahl, Don't ask, don't tell, but benzodiazepines are still the leading treatments for anxiety disorder. *J. Clin. Psychiatry* **63**, 756–757 (2002).
7. M. B. Stein, J. Sareen, Clinical practice. Generalized anxiety disorder. *N. Engl. J. Med.* **373**, 2059–2068 (2015).
8. V. Starcevic, The reappraisal of benzodiazepines in the treatment of anxiety and related disorders. *Expert Rev. Neurother.* **14**, 1275–1286 (2014).
9. C. A. Tassinari *et al*., The use of diazepam and clonazepam in epilepsy. *Epilepsia* **39**, S7–S14 (2007).
10. E. Trinka, F. Brigo, "Benzodiazepines used in the treatment of epilepsy" in *The Treatment of Epilepsy*, S. Shorvon, E. Perucca, J. Engel, Eds. (John Wiley & Sons, Ltd, 2015), pp. 398–417.
11. F. Brigo, N. L. Bragazzi, S. Bacigaluppi, R. Nardone, E. Trinka, Is intravenous lorazepam really more effective and safe than intravenous diazepam as first-line treatment for convulsive status epilepticus? A systematic review with meta-analysis of randomized controlled trials. *Epilepsy Behav.* **64**, 29–36 (2016).
12. B. L. Richards, S. L. Whittle, R. Buchbinder, Muscle relaxants for pain management in rheumatoid arthritis. *Cochrane Database Syst. Rev.* **1**, CD008922 (2012).
13. M. A. Schuckit, Recognition and management of withdrawal delirium (delirium tremens). *N. Engl. J. Med.* **371**, 2109–2113 (2014).
14. C. Braestrup, R. F. Squires, Specific benzodiazepine receptors in rat brain characterized by high-affinity (3H)diazepam binding. *Proc. Natl. Acad. Sci. U.S.A.* **74**, 3805–3809 (1977).
15. R. F. Squires, C. Brastrup, Benzodiazepine receptors in rat brain. *Nature* **266**, 732–734 (1977).
16. H. Möhler, T. Okada, Benzodiazepine receptor: Demonstration in the central nervous system. *Science* **198**, 849–851 (1977).
17. U. Rudolph *et al*., Benzodiazepine actions mediated by specific γ-aminobutyric acid(A) receptor subtypes. *Nature* **401**, 796–800 (1999).
18. I. Tobler, C. Kopp, T. Deboer, U. Rudolph, Diazepam-induced changes in sleep: Role of the α 1 GABA(A) receptor subtype. *Proc. Natl. Acad. Sci. U.S.A.* **98**, 6464–6469 (2001).
19. K. Löw *et al*., Molecular and neuronal substrate for the selective attenuation of anxiety. *Science* **290**, 131–134 (2000).
20. M. M. Savić *et al*., Are GABAA receptors containing α5 subunits contributing to the sedative properties of benzodiazepine site agonists? *Neuropsychopharmacology* **33**, 332–339 (2008).
21. N. G. Bowery, "Reflections on more than 30 years association with Hanns" in *Advances in Pharmacology*, U. Rudolph, Ed. (Academic Press, 2015), **vol. 73, chap. 1**, pp. 1–11.
22. F. Crestani, U. Rudolph, "Behavioral functions of GABAA receptor subtypes–The Zurich experience" in *Advances in Pharmacology*, U. Rudolph, Ed. (Academic Press, 2015), **vol. 72, chap. 2**, pp. 37–51.
23. K. Vogt, "Diversity in GABAergic signaling" in *Advances in Pharmacology*, U. Rudolph, Ed. (Academic Press, 2015), **vol. 73, chap. 8**, pp. 203–222.
24. M. Fagiolini *et al*., Specific GABAA circuits for visual cortical plasticity. *Science* **303**, 1681–1683 (2004).
25. S. Masiulis *et al*., $GABA_A$ receptor signalling mechanisms revealed by structural pharmacology. *Nature* **565**, 454–459 (2019).
26. P. S. Miller, A. R. Aricescu, Crystal structure of a human GABAA receptor. *Nature* **512**, 270–275 (2014).
27. J. H. Kehne, G. D. Maynard, "GABA and schizophrenia"in *Targets and Emerging Therapies for Schizophrenia*, J. S. Albert, M. W. Wood, Eds. (John Wiley & Sons, Inc., Hoboken, NJ, 2012), pp. 425–467.
28. S. Braat, R. F. Kooy, The GABAA receptor as a therapeutic target for neurodevelopmental disorders. *Neuron* **86**, 1119–1130 (2015).
29. H. T. Chao *et al*., Dysfunction in GABA signalling mediates autism-like stereotypies and Rett syndrome phenotypes. *Nature* **468**, 263–269 (2010).
30. A. K. Shetty, A. Bates, Potential of GABA-ergic cell therapy for schizophrenia, neuropathic pain, and Alzheimer's and Parkinson's diseases. *Brain Res.* **1638**, 74–87 (2016).
31. H. Möhler, The GABA system in anxiety and depression and its therapeutic potential. *Neuropharmacology* **62**, 42–53 (2012).
32. G. Northoff, E. Sibille, Why are cortical GABA neurons relevant to internal focus in depression? A cross-level model linking cellular, biochemical and neural network findings. *Mol. Psychiatry* **19**, 966–977 (2014).
33. A. A. Zurek *et al*., Sustained increase in α5GABAA receptor function impairs memory after anesthesia. *J. Clin. Invest.* **124**, 5437–5441 (2014).
34. S. G. Brickley, I. Mody, Extrasynaptic GABA(A) receptors: Their function in the CNS and implications for disease. *Neuron* **73**, 23–34 (2012).
35. U. Rudolph, F. Knoflach, Beyond classical benzodiazepines: Novel therapeutic potential of GABAA receptor subtypes. *Nat. Rev. Drug Discov.* **10**, 685–697 (2011).
36. S. R. Adams, R. Y. Tsien, Controlling cell chemistry with caged compounds. *Annu. Rev. Physiol.* **55**, 755–784 (1993).
37. G. Mayer, A. Heckel, Biologically active molecules with a "light switch". *Angew. Chem. Int. Ed. Engl.* **45**, 4900–4921 (2006).
38. G. C. Ellis-Davies, Caged compounds: Photorelease technology for control of cellular chemistry and physiology. *Nat. Methods* **4**, 619–628 (2007).
39. N. Ankenbruck, T. Courtney, Y. Naro, A. Deiters, Optochemical control of biological processes in cells and animals. *Angew. Chem. Int. Ed. Engl.* **57**, 2768–2798 (2018).
40. K. Hüll, J. Morstein, D. Trauner, In vivo photopharmacology. *Chem. Rev.* **118**, 10710–10747 (2018).
41. M. Wilcox *et al*., Synthesis of photolabile precursors of amino acid neurotransmitters. *J. Org. Chem.* **55**, 1585–1589 (1990).
42. K. R. Gee, R. Wieboldt, G. P. Hess, Synthesis and photochemistry of a new photolabile derivative of GABA-neurotransmitter release and receptor activation in the microsecond time region. *J. Am. Chem. Soc.* **116**, 8366–8367 (1994).
43. D. D. Shi, F. F. Trigo, M. F. Semmelhack, S. S. Wang, Synthesis and biological evaluation of bis-CNB-GABA, a photoactivatable neurotransmitter with low receptor interference and chemical two-photon uncaging properties. *J. Am. Chem. Soc.* **136**, 1976–1981 (2014).
44. M. Canepari, L. Nelson, G. Papageorgiou, J. E. T. Corrie, D. Ogden, Photochemical and pharmacological evaluation of 7-nitroindolinyl-and 4-methoxy-7-nitroindolinyl-amino acids as novel, fast caged neurotransmitters. *J. Neurosci. Methods* **112**, 29–42 (2001).
45. L. Zayat, M. Salierno, R. Etchenique, Ruthenium(II) bipyridyl complexes as photolabile caging groups for amines. *Inorg. Chem.* **45**, 1728–1731 (2006).
46. L. Zayat *et al*., A new inorganic photolabile protecting group for highly efficient visible light GABA uncaging. *ChemBioChem* **8**, 2035–2038 (2007).
47. M. T. Richers, J. M. Amatrudo, J. P. Olson, G. C. Ellis-Davies, Cloaked caged compounds: Chemical probes for two-photon optoneurobiology. *Angew. Chem. Int. Ed. Engl.* **56**, 193–197 (2017).
48. J. M. Amatrudo *et al*., Wavelength-selective one- and two-photon uncaging of GABA. *ACS Chem. Neurosci.* **5**, 64–70 (2014).
49. E. M. Rial Verde, L. Zayat, R. Etchenique, R. Yuste, Photorelease of GABA with visible light using an inorganic caging group. *Front. Neural Circuits* **2**, 2 (2008).
50. P. Molnár, J. V. Nadler, gamma-Aminobutyrate, alpha-carboxy-2-nitrobenzyl ester selectively blocks inhibitory synaptic transmission in rat dentate gyrus. *Eur. J. Pharmacol.* **391**, 255–262 (2000).
51. S. S. H. Wang, G. J. Augustine, Confocal imaging and local photolysis of caged compounds: Dual probes of synaptic function. *Neuron* **15**, 755–760 (1995).
52. F. F. Trigo, G. Papageorgiou, J. E. T. Corrie, D. Ogden, Laser photolysis of DPNI-GABA, a tool for investigating the properties and distribution of GABA receptors and for silencing neurons in situ. *J. Neurosci. Methods* **181**, 159–169 (2009).
53. S. Kantevari, M. Matsuzaki, Y. Kanemoto, H. Kasai, G. C. Ellis-Davies, Two-color, two-photon uncaging of glutamate and GABA. *Nat. Methods* **7**, 123–125 (2010).
54. X. Yang, D. L. Rode, D. S. Peterka, R. Yuste, S. M. Rothman, Optical control of focal epilepsy in vivo with caged γ-aminobutyric acid. *Ann. Neurol.* **71**, 68–75 (2012).
55. M. T. Richers, S. Passlick, H. Agarwal, G. C. R. Ellis-Davies, Dendrimer conjugation enables multiphoton chemical neurophysiology with an extended π-electron caging chromophore. *Angew Chem. Int. Ed. Engl.* **58**, 12086–12090 (2019).
56. W.-C. Lin *et al*., Engineering a light-regulated GABAA receptor for optical control of neural inhibition. *ACS Chem. Biol.* **9**, 1414–1419 (2014).
57. W.-C. Lin *et al*., A comprehensive optogenetic pharmacology toolkit for in vivo control of GABA(A) receptors and synaptic inhibition. *Neuron* **88**, 879–891 (2015).
58. W.-C. Lin, M.-C. Tsai, R. Rajappa, R. H. Kramer, Design of a highly bistable photoswitchable tethered ligand for rapid and sustained manipulation of neurotransmission. *J. Am. Chem. Soc.* **140**, 7445–7448 (2018).

59. R. Huckvale, M. Mortensen, D. Pryde, T. G. Smart, J. R. Baker, Azogabazine; a photochromic antagonist of the GABAA receptor. *Org. Biomol. Chem.* **14**, 6676–6678 (2016).
60. G. Maleeva *et al*., A photoswitchable GABA receptor channel blocker. *Br. J. Pharmacol.* **176**, 2661–2677 (2019).
61. M. Stein *et al*., Azo-propofols: Photochromic potentiators of GABA(A) receptors. *Angew. Chem. Int. Ed. Engl.* **51**, 10500–10504 (2012).
62. L. Yue *et al*., Robust photoregulation of GABA(A) receptors by allosteric modulation with a propofol analogue. *Nat. Commun.* **3**, 1095 (2012).
63. P. Paoletti, G. C. R. Ellis-Davies, A. Mourot, Optical control of neuronal ion channels and receptors. *Nat. Rev. Neurosci.* **20**, 514–532 (2019).
64. L. N. Eisenman *et al*., Anticonvulsant and anesthetic effects of a fluorescent neurosteroid analog activated by visible light. *Nat. Neurosci.* **10**, 523–530 (2007).
65. P. Bregestovski, G. Maleeva, P. Gorostiza, Light-induced regulation of ligand-gated channel activity. *Br. J. Pharmacol.* **175**, 1892–1902 (2018).
66. M. E. Derieg *et al*., The reaction of epoxides with 1,4-benzodiazepines, mechanism and structural assignments. *Tetrahedron* **27**, 2591–2598 (1971).
67. T. L. Lemke, A. R. Hanze, The synthesis of oxazolo- and oxazino[3,2-d] [1,4] benzodiazepinones. *J. Heterocycl. Chem.* **8**, 125–128 (1971).
68. T. Miyadera *et al*., Anxiolytic sedatives. 1. Synthesis and pharmacology of benzo[6,7]-1,4-diazepino[5,4-b]oxazole derivatives and analogs. *J. Med. Chem.* **14**, 520–526 (1971).
69. L. H. Sternbach, 1,4-benzodiazepines. Chemistry and some aspects of the structure-activity relationship. *Angew. Chem. Int. Ed. Engl.* **10**, 34–43 (1971).
70. J. Vida, J. Yevich, "Sedative-hypnotics" in *Burger's Medicinal Chemistry and Drug Discovery*, Donald J. Abraham, Ed. (John Wiley & Sons, Inc., Hoboken, NJ, 2003), pp. 201–261. (2003).
71. Q. Huang *et al*., Pharmacophore/receptor models for GABA(A)/BzR subtypes ($\alpha1\beta3\gamma2$, $\alpha5\beta3\gamma2$, and $\alpha6\beta3\gamma2$) via a comprehensive ligand-mapping approach. *J. Med. Chem.* **43**, 71–95 (2000).
72. Y. Zhang, S. Tang, L. Sansalone, J. D. Baker, F. M. Raymo, A photoswitchable fluorophore for the real-time monitoring of dynamic events in living organisms. *Chemistry* **22**, 15027–15034 (2016).
73. L. Sansalone *et al*., A photoactivatable far-red/near-infrared BODIPY to monitor cellular dynamics in vivo. *ACS Sens.* **3**, 1347–1353 (2018).
74. S. Tang, B. Donaphon, M. Levitus, F. M. Raymo, Structural implications on the properties of self-assembling supramolecular hosts for fluorescent guests. *Langmuir* **32**, 8676–8687 (2016).
75. M. H. Kang-Park, W. A. Wilson, S. D. Moore, Differential actions of diazepam and zolpidem in basolateral and central amygdala nuclei. *Neuropharmacology* **46**, 1–9 (2004).
76. A. N. Shrivastava, A. Triller, W. Sieghart, GABA(A) receptors: Post-synaptic co-localization and cross-talk with other receptors. *Front. Cell. Neurosci.* **5**, 7 (2011).
77. W. M. Connelly *et al*., GABAB receptors regulate extrasynaptic GABAA receptors. *J. Neurosci.* **33**, 3780–3785 (2013).
78. W. Tao, M. H. Higgs, W. J. Spain, C. B. Ransom, Postsynaptic GABAB receptors enhance extrasynaptic GABAA receptor function in dentate gyrus granule cells. *J. Neurosci.* **33**, 3738–3743 (2013).
79. F. F. Trigo, J. E. T. Corrie, D. Ogden, Laser photolysis of caged compounds at 405 nm: Photochemical advantages, localisation, phototoxicity and methods for calibration. *J. Neurosci. Methods* **180**, 9–21 (2009).
80. L. G. Aguayo, F. C. Pancetti, R. L. Klein, R. A. Harris, Differential effects of GABAergic ligands in mouse and rat hippocampal neurons. *Brain Res.* **647**, 97–105 (1994).
81. E. B. Brown, J. B. Shear, S. R. Adams, R. Y. Tsien, W. W. Webb, Photolysis of caged calcium in femtoliter volumes using two-photon excitation. *Biophys. J.* **76**, 489–499 (1999).
82. R. Wieboldt, D. Ramesh, B. K. Carpenter, G. P. Hess, Synthesis and photochemistry of photolabile derivatives of gamma-aminobutyric acid for chemical kinetic investigations of the gamma-aminobutyric acid receptor in the millisecond time region. *Biochemistry* **33**, 1526–1533 (1994).
83. N. Hájos, Z. Nusser, E. A. Rancz, T. F. Freund, I. Mody, Cell type- and synapse-specific variability in synaptic GABAA receptor occupancy. *Eur. J. Neurosci.* **12**, 810–818 (2000).
84. J. C. Poncer, R. Dürr, B. H. Gähwiler, S. M. Thompson, Modulation of synaptic GABAA receptor function by benzodiazepines in area CA3 of rat hippocampal slice cultures. *Neuropharmacology* **35**, 1169–1179 (1996).
85. A. S. Cohen, D. D. Lin, G. L. Quirk, D. A. Coulter, Dentate granule cell GABA(A) receptors in epileptic hippocampus: Enhanced synaptic efficacy and altered pharmacology. *Eur. J. Neurosci.* **17**, 1607–1616 (2003).
86. C. Leroy, P. Poisbeau, A. F. Keller, A. Nehlig, Pharmacological plasticity of GABA(A) receptors at dentate gyrus synapses in a rat model of temporal lobe epilepsy. *J. Physiol.* **557**, 473–487 (2004).
87. I. Mody, Y. De Koninck, T. S. Otis, I. Soltesz, Bridging the cleft at GABA synapses in the brain. *Trends Neurosci.* **17**, 517–525 (1994).
88. C. J. Rogers, R. E. Twyman, R. L. Macdonald, Benzodiazepine and beta-carboline regulation of single GABAA receptor channels of mouse spinal neurones in culture. *J. Physiol.* **475**, 69–82 (1994).
89. A. M. Lavoie, R. E. Twyman, Direct evidence for diazepam modulation of GABAA receptor microscopic affinity. *Neuropharmacology* **35**, 1383–1392 (1996).
90. A. S. Cohen, D. D. Lin, D. A. Coulter, Protracted postnatal development of inhibitory synaptic transmission in rat hippocampal area CA1 neurons. *J. Neurophysiol.* **84**, 2465–2476 (2000).
91. D. Perrais, N. Ropert, Effect of zolpidem on miniature IPSCs and occupancy of post-synaptic GABAA receptors in central synapses. *J. Neurosci.* **19**, 578–588 (1999).
92. E. Engin, R. S. Benham, U. Rudolph, An emerging circuit pharmacology of $GABA_A$ receptors. *Trends Pharmacol. Sci.* **39**, 710–732 (2018).
93. National Research Council, *Guide for the Care and Use of Laboratory Animals* (National Academies Press, Washington, DC, ed. 8, 2011).